ACADEMIA ROMÂNĂ
Revue Roumaine de Chimie
http://web.icf.ro/rrch/

Rev. Roum. Chim.,
2018, *63*(12), 1115-1122

PREPARATION, STRUCTURE, PHOTOLUMINESCENT, MAGNETIC AND SEMICONDUCTIVE PROPERTIES OF A PRASEODYMIUM COMPLEX WITH A TWO-DIMENSIONAL MOTIF

Qiu-Yan LUO,[a] Wen-Tong CHEN,[a,b]* Jian-Gen HUANG,[a] Yin-Feng WANG[a] and Ding-Wa ZHANG[a]

[a]Institute of Applied Chemistry, Jiangxi Province Key Laboratory of Coordination Chemistry, School of Chemistry and Chemical Engineering, Jinggangshan University, Ji'an, Jiangxi 343009, China
[b]State Key Laboratory of Structural Chemistry, Fujian Institute of Research on the Structure of Matter, Chinese Academy of Sciences, Fuzhou, Fujian 350002, China

Received August 16, 2017

A praseodymium complex, $[Pr_2(C_2O_4)_3(H_2O)_6]_n \cdot 2n$MeOH$\cdot 2n$EtOH (**1**), has been synthesized through a solvothermal reaction and structurally characterized by single crystal X-ray diffraction. Complex **1** is crystallized in the space group $P2_1/c$ of the monoclinic system with two formula units in one cell. It is characteristic of a two-dimensional (2D) structure with the praseodymium atom binding with nine oxygen atoms to give a tricapped trigonal prismatic coordination geometry. The $[Pr_2(C_2O_4)_3(H_2O)_6]_n$ layers, methanol and ethanol molecules interconnect together through abundant hydrogen-bonding interactions to yield a three-dimensional (3D) supramolecular framework. Photoluminescence measurements with solid-state sample discover that it has an emission in the green region. The photoluminescent bands at 512, 526, 547, 560 and 582 nm are attributable to the distinct emission $^3P_0$-^3H_J (J = 4, 5, 6) and $^3P_0$-^3F_J (J = 2, 3) transitions of the Pr^{3+} ion. Diffuse reflectance measurement with solid-state sample reveals the existence of a narrow optical band gap of 1.46 eV. Variable-temperature magnetic susceptibility and field dependence magnetization measurements are also investigated and the magnetic susceptibility obeys the Curie-Weiss law ($\chi_m = c/(T-\theta)$) with the value C being of 2.45 K and Weiss constant θ being of –21.67 K.

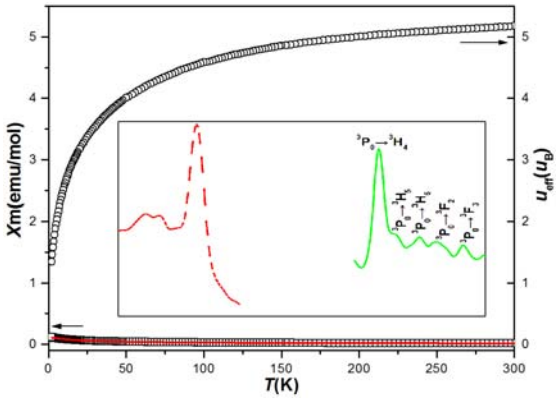

INTRODUCTION

Lanthanide complexes often exhibit special optical and magnetic properties owing to the presence of 4*f* electrons of the lanthanide ions. Lanthanide complexes are particularly desirable for their magnetic, photoluminescent, chemical, and electronic characteristics originating from the 4*f* electrons. Nowadays, lanthanide complexes have become a significant research hotspot due to their interesting structural motifs, abundant properties and extensive application values in the fields like light-emitting materials, sensors, electroluminescent devices, fluorescent probes, magnetic materials, cell imaging, and analysis test, and so on.[1-4] A large number of lanthanide complexes have thus far been prepared.[5-9] As one of the members of lanthanide, praseodymium is also an interesting element because praseodymium compounds can generally display different ground state properties due to the vital role of quadrupolar fluctuations and crystalline-electric-field effects.[10,11] Furthermore, the trivalent praseodymium ion is very useful for visible fiber lasers because it can afford efficient energy conversion, good beam quality, pliable configurations, small footprint, and

* Corresponding author: wtchen@jgsu.edu.cn

wideband transitions. To our knowledge, investigation on the praseodymium complexes is relatively rare up to date. Therefore, the structures and properties of praseodymium complexes have yet to be explored. In order to obtain new lanthanide complexes with novel structures and properties, we recently focus on the synthesis and characterization of praseodymium complexes. We report in this work the solvothermal preparation, crystal structure, photoluminescent, magnetic and semiconductive properties of a new praseodymium complex, $[Pr_2(C_2O_4)_3(H_2O)_6]_n \cdot 2n$MeOH$\cdot 2n$EtOH (**1**), which is characteristic of a 2D layer and a 3D supramolecular framework, although this structural type was already reported.[12,13]

EXPERIMENTAL

Synthesis and characterization of $[Pr_2(C_2O_4)_3(H_2O)_6]_n \cdot 2n$MeOH$\cdot 2n$EtOH (1): All the chemicals and reagents are of analytical grade, commercially obtained and used without further purification. It was synthesized by mixing $Pr(NO_3)_3 \cdot 6H_2O$ (1 mmol, 434 mg), 5-sulfosalicylic acid dehydrate (2 mmol, 434 mg), 1 mL methanol, 1 mL ethanol and 10 mL distilled water in a 25 mL Teflon-lined stainless steel autoclave and heated at 453 K for 15 days, then power off. When the autoclaves were cooled down to room temperature, yellow block crystals were obtained and applied to single crystal X-ray analysis. The yield is 26% based on praseodymium. $C_{12}H_{32}O_{22}Pr_2$: calcd. C, 17.79; H, 3.98; Found C, 17.92; H, 4.03. Elemental microanalyses of carbon and hydrogen were carried out with an Elementar Vario EL elemental analyzer. Photoluminescent experiments were carried out with solid-state sample at room temperature on a F97XP spectrometer. Solid-state UV/vis spectra with powder sample were recorded at room temperature on a computer-controlled TU1901 UV/vis spectrometer equipped with an integrating sphere in the wavelength range of 190–900 nm. $BaSO_4$ powder was applied as a 100% reflectance reference, on which the ground powder samples were coated. Variable-temperature magnetic susceptibility and field dependence magnetization measurements of **1** on polycrystalline samples were conducted on a MPMS Quantum Design SQUID magnetometer. All the magnetic data were corrected for diamagnetism estimated from the Pascal's constants.

X-ray crystallographic study: The intensity data set were collected on a SuperNova CCD X-ray diffractometer with a carefully selected single crystal. The X-ray source is graphite monochromated Mo-$K\alpha$ radiation (λ = 0.71073 Å). The data reduction and empirical absorption correction were performed with the CrystalClear software.[14] The crystal structure was solved by using the direct method and the Siemens SHELXTL™ V5 software[15] and refined by using a full-matrix least-squares refinement on F^2. All the non-hydrogen atoms were found on the difference Fourier maps and applied anisotropic refinement. The hydrogen atoms were theoretically added to their parent atoms and included in the structural factor calculation with assigned isotropic thermal parameters. The crystal data as well as the details of data collection and refinement are given in Table 1, while the selected bond lengths and bond angles were presented in Table 2. Crystallographic data for the structural analysis have been deposited with the Cambridge Crystallographic Data Centre, CCDC No. 1565375. Copies of this information may be obtained free of charge from the Director, CCDC, 12 Union Road, Cambridge, CBZ 1EZ, UK (Fax: +44-1223-336033; email: deposit@ccdc.cam.ac.uk or www:http://www.ccdc. cam.ac.uk).

Table 1

Crystal data and structure refinement details

Formula	$C_{12}H_{32}O_{22}Pr_2$
Mr	810.20
color	yellow
Crystal size/mm^3	0.17 0.12 0.10
Crystal system	monoclinic
Space group	$P2_1/c$
a (Å)	11.2551(3)
b (Å)	9.6369(2)
c (Å)	10.3403(3)
β (°)	114.537(3)
V (Å^3)	1020.27(5)
Z	2
$2\theta_{max}$ (°)	50
Reflections collected	5842
Independent, observed reflections (R_{int})	1800, 1715 (0.0288)
$d_{calcd.}$ (g/cm^3)	2.637
μ (mm^{-1})	4.837
T (K)	293(2)
F(000)	796
R^1, wR^2	0.0283, 0.0822
S	1.002
Largest and Mean Δ/σ	0, 0
$\Delta\rho$ (max, min) (e/Å^3)	0.784, -1.053

Table 2

Selected bond lengths (Å) and bond angles (º)

Pr(1)-O(1)#1	2.476(4)	O(3W)-Pr(1)-O(5)#3	95.12(15)
Pr(1)-O(2)	2.528(4)	O(4)-Pr(1)-O(5)#3	137.70(12)
Pr(1)-O(3)#2	2.477(3)	O(1)#1-Pr(1)-O(2)	64.57(12)
Pr(1)-O(4)	2.520(4)	O(3)#2-Pr(1)-O(2)	144.63(13)
Pr(1)-O(5)#3	2.526(4)	O(2W)-Pr(1)-O(2)	127.09(13)
Pr(1)-O(6)	2.586(4)	O(3W)-Pr(1)-O(2)	75.18(13)
Pr(1)-O(1W)	2.546(4)	O(4)-Pr(1)-O(2)	124.50(12)
Pr(1)-O(2W)	2.502(4)	O(5)#3-Pr(1)-O(2)	69.88(13)
Pr(1)-O(3W)	2.502(4)	O(1)#1-Pr(1)-O(1W)	83.31(16)
		O(3)#2-Pr(1)-O(1W)	81.06(14)
O(1)#1-Pr(1)-O(3)#2	136.38(12)	O(2W)-Pr(1)-O(1W)	136.76(15)
O(1)#1-Pr(1)-O(2W)	76.05(14)	O(3W)-Pr(1)-O(1W)	71.86(17)
O(3)#2-Pr(1)-O(2W)	88.27(14)	O(4)-Pr(1)-O(1W)	69.17(14)
O(1)#1-Pr(1)-O(3W)	137.38(13)	O(5)#3-Pr(1)-O(1W)	142.94(13)
O(3)#2-Pr(1)-O(3W)	73.97(14)	O(2)-Pr(1)-O(1W)	73.23(13)
O(2W)-Pr(1)-O(3W)	144.15(16)	O(1)#1-Pr(1)-O(6)	140.75(14)
O(1)#1-Pr(1)-O(4)	71.75(12)	O(3)#2-Pr(1)-O(6)	67.15(12)
O(3)#2-Pr(1)-O(4)	64.64(12)	O(2W)-Pr(1)-O(6)	73.95(14)
O(2W)-Pr(1)-O(4)	68.40(13)	O(3W)-Pr(1)-O(6)	70.50(15)
O(3W)-Pr(1)-O(4)	126.18(15)	O(4)-Pr(1)-O(6)	118.21(13)
O(1)#1-Pr(1)-O(5)#3	84.18(13)	O(5)#3-Pr(1)-O(6)	62.99(12)
O(3)#2-Pr(1)-O(5)#3	129.69(13)	O(2)-Pr(1)-O(6)	117.25(12)
O(2W)-Pr(1)-O(5)#3	72.38(13)	O(1W)-Pr(1)-O(6)	135.88(15)

Symmetry transformations used to generate equivalent atoms: #1 -*x*+2, -*y*+1, -*z*+1; #2 -*x*+1, -*y*+1, -*z*; #3 -*x*+2, -*y*+1, -*z*.

RESULTS AND DISCUSSION

Crystal Structure

Single crystal X-ray diffraction analyses show that complex **1** is composed of neutral 2D $[Pr_2(C_2O_4)_3(H_2O)_6]_n$ layers, isolated methanol and ethanol molecules, as depicted in Fig. 1. Complex **1** is crystallized in the $P2_1/c$ space group of the monoclinic system with two formular units in one cell. Each praseodymium atom is coordinated by nine oxygen atoms, of which six are from three oxalate groups and three are from three coordination water molecule, to give a tricapped trigonal prismic coordination geometry. The bond lengths of Pr–O are in the range of 2.476(4) Å – 2.586(4) Å with an average value of 2.518(4) Å, which are in the normal range and comparable with those reported in the references.[16-21] The result of the bond valence calculation reveals that the praseodymium ion is in a 3+ oxidation state (Pr1: 3.208).[22] In the title complex, all the oxalate groups act as a quadridentate ligand. Each oxalate anion chelates to two praseodymium ions with the chelating angles in the range of 62.9(1)°–64.6(1)°. Six oxalate groups interconnect six praseodymium ions together to yield a ring (Fig. 2a). Each ring links to six neighboring ones and extends along the ac plane to give a planar 2D layer (Fig. 2). The neighboring Pr···Pr distance in the ring is 6.4505(4) Å, 6.4593(4) Å, 6.5865(5) Å, 6.4505(4) Å, 6.4593(4) Å, 6.5865(5) Å. The $[Pr_2(C_2O_4)_3(H_2O)_6]_n$ layers, methanol and ethanol molecules interconnect together through abundant O-H···O and C-H···O hydrogen-bonding interactions to yield a 3D supramolecular framework, as shown in Fig. 3.

Photoluminescence Spectrum

It is well known that lanthanide complexes have distinct photoluminescent emission bands due to their rich *f*-orbital configurations. Lanthanide ions have an important feature that they can display strong photoluminescence and ability of tuning their emission range for specific applications in different regions of the spectrum. Amongst the lanthanide ions, trivalent praseodymium ion (Pr^{3+}) has been studied extensively for its potential applications at the fields of infrared lasers, sensors, photonics, electronics, and special band amplification. Pr^{3+}-containing complexes are studied for optical imaging because the Pr^{3+} energy level scheme contains some metastable multiplets. Based on the above consideration and in order to reveal the potential photoluminescent properties, we carried out the photoluminescent measurements for complex **1** in the solid state at room temperature. The experiment result of the photoluminescent measurements is shown in Fig. 4. It is clearly that the photoluminescent spectrum of complex **1** exhibits an effective energy absorption locating in the wavelength range of 300–400 nm. Upon the emission of 512 nm, the excitation peaks have a main band at 363 nm, accompanied by two

smaller peaks at 321 nm and 333 nm, respectively. We then also carried out the corresponding photoluminescent emission spectrum of complex **1**, upon excited by the wavelength of 363 nm. The emission spectrum is characteristic of a main peak at 512 nm in the green region as well as four shoulder peaks at 526, 547, 560 and 582 nm, respectively. It is proposed that the photoluminescent peaks at 512, 526, 547, 560 and 582 nm are attributable to the distinct emission $^3P_0$-^3H_J (J = 4, 5, 6) and $^3P_0$-^3F_J (J = 2, 3) transitions of the Pr^{3+} ion. This indicates that effective energy transfer happened and a conjugated system is established between the oxalate groups and the Pr^{3+} ion. Therefore, complex **1** can be a potential green photoluminescence material.

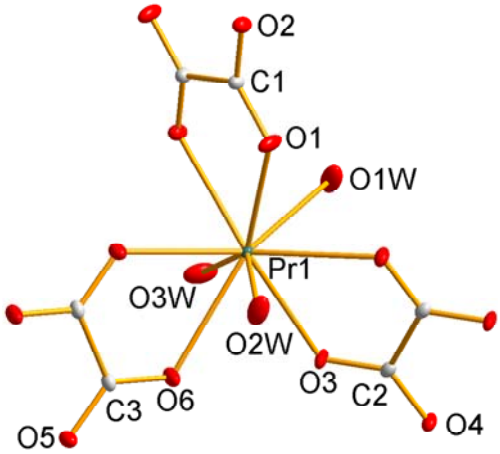

Fig. 1 – An ORTEP drawing of **1** with 30% thermal ellipsoids.
Lattice methanol and ethanol molecules and hydrogen atoms were omitted for clarity.

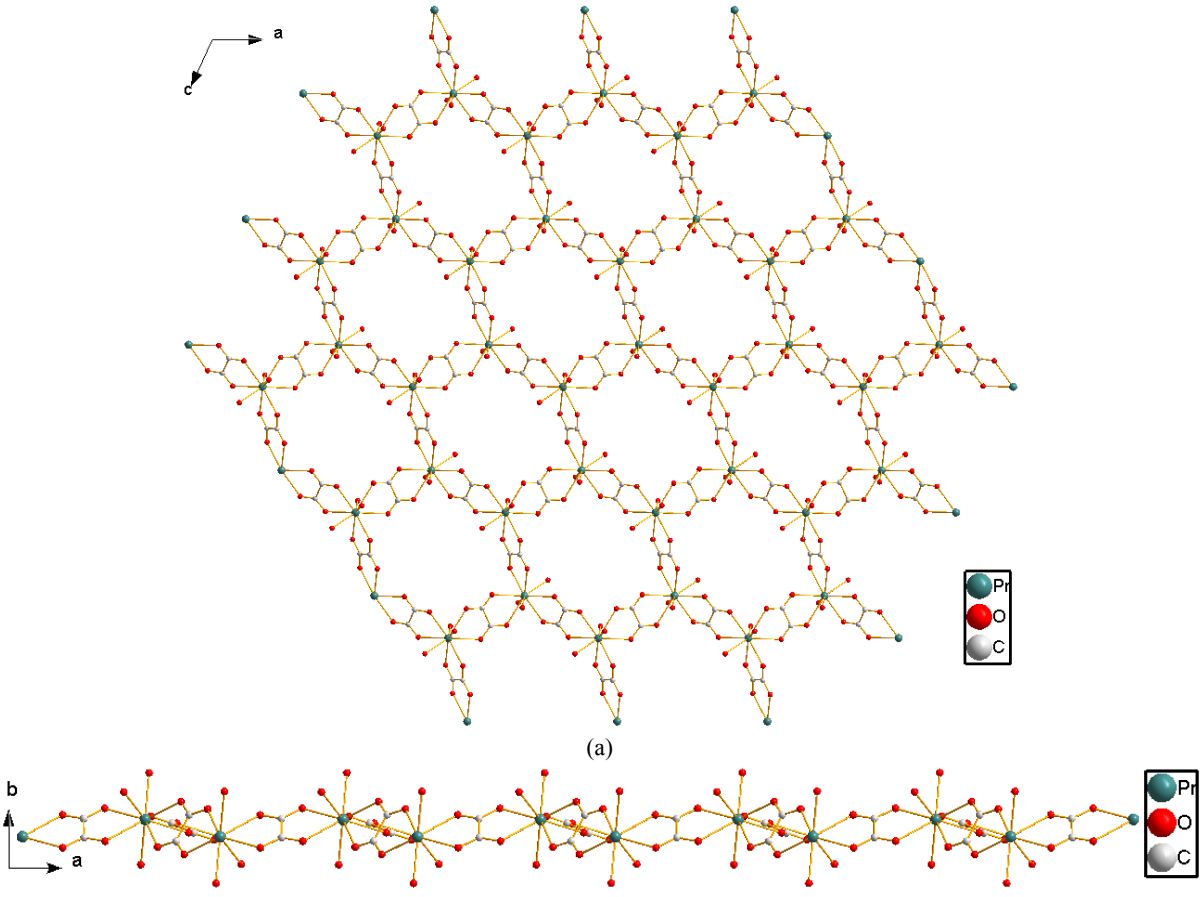

Fig. 2 – The 2D layer viewed from different directions.

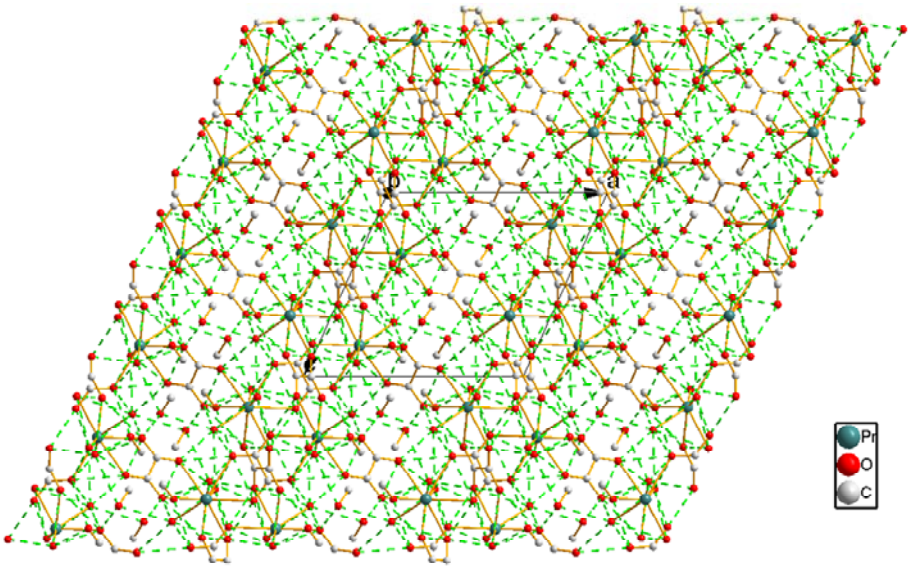

Fig. 3 – A packing diagram of **1** with the dashed lines representing the hydrogen bonding interactions (Å, º): O1W-H1WA···O7(1-*x*, 1/2+*y*, 1/2-*z*) 2.863(14), 163; O2W-H2WA···O2(2-*x*, -1/2+*y*, 1/2-*z*) 2.818(6), 162; O3W-H3WA···O5(*x*, 3/2-*y*, 1/2+*z*) 2.699(6), 164; C5-H5A···O7(1-*x*, -*y*, -*z*) 2.82(4), 149; C5-H5A···O8(1-*x*, -*y*, -*z*) 2.81(5), 115; C5-H5B···O3W(*x*, -1+*y*, *z*) 2.82(4), 137; C5-H5B···O1W(*x*, 1/2-*y*, -1/2+*z*) 2.60(4), 107; C5-H5C···O4(*x*, 1/2-*y*, -1/2+*z*) 3.12(4), 128.

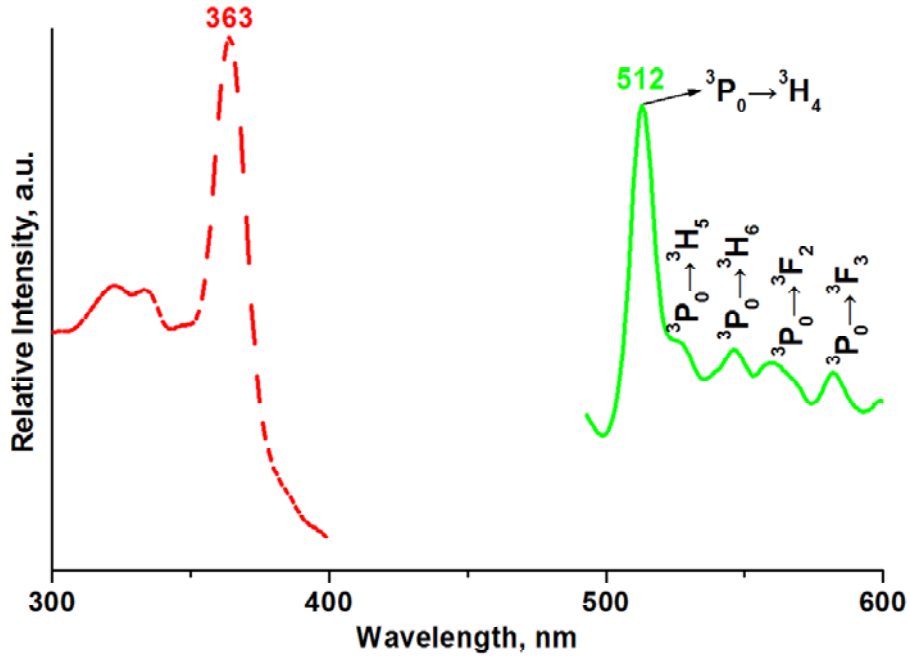

Fig. 4 – Solid-state photoluminescent spectra of **1** measured at room temperature. Red: excitation; green: emission.

Solid-state UV/vis Diffuse Reflectance Spectrum

Solid-state UV/vis diffuse reflectance spectra of complex **1** with powder sample were recorded at room temperature. The diffuse reflectance spectra data were treated with the well-known Kubelka-Munk function, namely, $\alpha/S = (1-R)^2/2R$. The parameter α of this function means the absorption coefficient, S refers to the scattering coefficient which is practically wavelength independent if the particle diameter is larger than 5 μm, while R is the reflectance. The value of the optical band gap can be determined by extrapolating from the linear portion of the absorption edges from the α/S vs. energy diagram. The solid-state diffuse reflectance spectrum reveals that complex **1** exhibits a narrow optical band gap of 1.46 eV, as presented in Fig. 5. As a result, complex **1** can be a candidate for narrow band gap semiconductors. The mild slope of the optical absorption edge of complex **1**

suggests that it could be an indirect transition.[23] The optical band gap of 1.46 eV of complex **1** is very close to those of GaAs (1.4 eV), CdTe (1.5 eV) and $CuInS_2$ (1.55 eV), all of the them are well-known as highly efficient photovoltaic compounds.[24, 25]

Magnetic Properties

Trivalent praseodymium ion (Pr^{3+})-containing complexes are supposed to generally possess magnetic behaviors. Therefore, the variable-temperature magnetic susceptibility and field dependence magnetization measurements of complex **1** on polycrystalline samples were carried out. Fig. 6 presents the thermal dependence of χ_M and μ_{eff} for **1**, where χ_m is the magnetic susceptibility per Pr-containing molecule. The red line corresponds to the theoretical line based on the Curie-Weiss model. When the temperature is decreased from 300 K to 50K, the χ_M vs T diagram nearly keeps horizontal, then the χ_M tardily increases when the temperature is further cooled down to 2 K with the χ_M being of 0.11 emu·mol^{-1}. The diagram of χ_M vs T of complex **1** displays an antiferromagnetic-like behavior. The essence of this antiferromagnetic-like behavior is unclear yet, but it is supposed to be relevant to the progressive thermal depopulation of the Stark components of the Pr^{III} ion. The magnetic susceptibility obeys well the Curie-Weiss equation ($\chi_m = c/(T-\theta)$) with C = 2.45 K and a negative Weiss constant θ = –21.67 K; this verifies the presence of antiferromagnetic-like interaction in complex **1**, which is in good agreement with the analogs.[26, 27] This antiferromagnetic-like interaction is the most probable the thermal depopulation of the Stark levels. The experimental μ_{eff} value is 5.09 μ_B which is larger than the 3.62 μ_B that would be expected for an isolated magnetic center of Pr^{3+} in complex **1**. As shown in Fig. 7, the field dependence magnetization measurement of complex **1** was performed at 2 K, showing a large coercive field of about 290 Oe and remnant magnetization of about 1.9×10^{-3} $N\beta$. The magnetization diagram increases gently with the increased field. The M vs H curve discovers that the magnetization is not saturated when the field is increased to 8 T with a value of about 0.42 Nβ.

CONCLUSIONS

In summary, a praseodymium complex was prepared and it is characterized by a 2D layer and a 3D supramolecular network. Solid-state photoluminescence experiments reveal that it shows an emission in the green region. The photoluminescent bands at 512, 526, 547, 560 and 582 nm are ascribed to the characteristic emission $^3P_0$-^3H_J (J = 4, 5, 6) and $^3P_0$-^3F_J (J = 2, 3) transitions of the Pr^{3+} ion. Solid-state UV/vis diffuse reflectance spectra reveals the existence of a narrow optical band gap of 1.46 eV. Variable-temperature magnetic susceptibility measurement shows the presence of antiferromagnetic interactions.

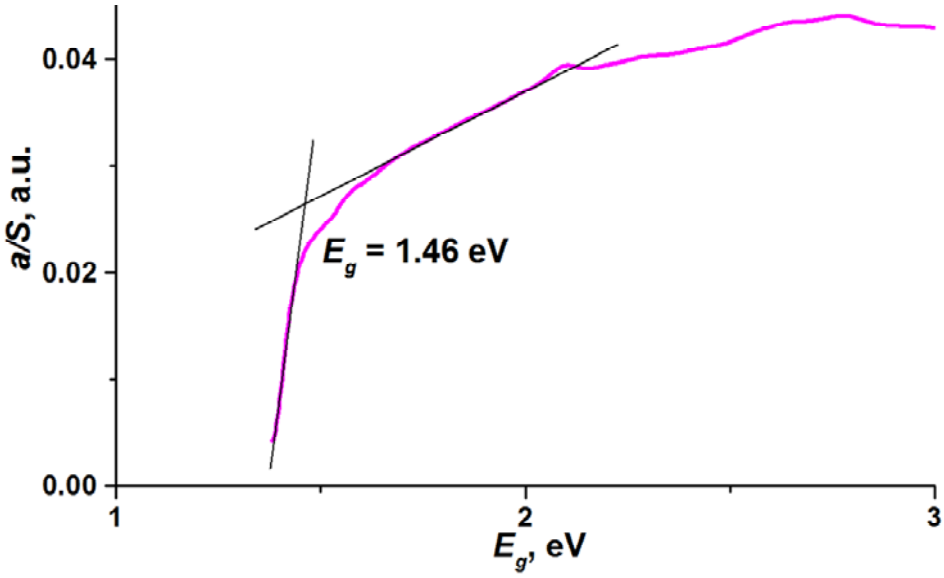

Fig. 5 – Solid-state diffuse reflectance spectrum for **1**.

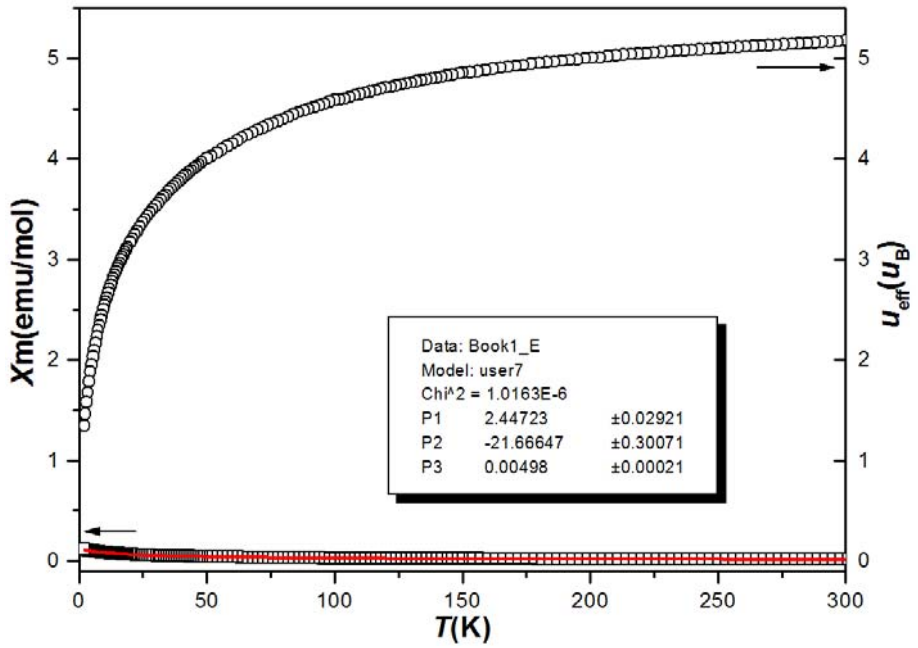

Fig. 6 – Thermal dependence of χ_M and μ_{eff} for **1**. The red line corresponds to the theoretical line based on the Curie-Weiss model.

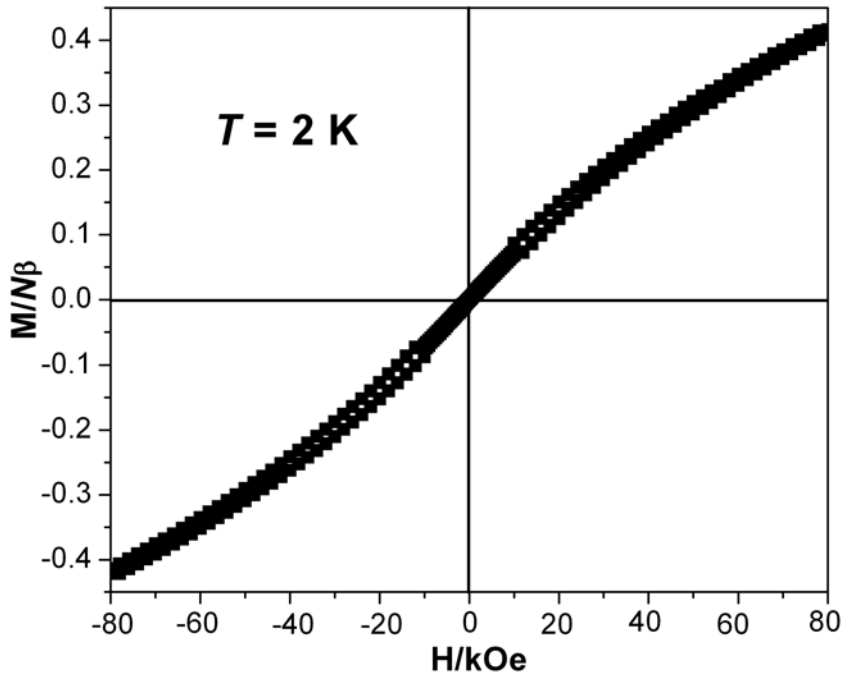

Fig. 7 – Magnetization vs *H* of **1**.

Acknowledgements: We gratefully acknowledge the financial support of the NSF of China (21361013, 21362015, 21461013), Jiangxi Provincial Science and Technology Support Key Project (20152ACG70021), Jiangxi Provincial Natural Science Foundation (20142BAB205062, 20133ACB20010), Jiangxi Provincial Department of Education's Item of Science and Technology(GJJ150761, GJJ14557, GJJ170637), Jinggangshan University Natural Science Item (JZ0813), and the open foundation (20150019, 20180008) of the State Key Laboratory of Structural Chemistry, Fujian Institute of Research on the Structure of Matter, Chinese Academy of Sciences.

REFERENCES

1. P. K. Chen, Q. C. Li, S. Grindy and N. H. Andersen, *J. Am. Chem. Soc.*, **2015**, *137*, 11590.
2. X. H. Zhou, L. Li, H. H. Li, A. Li, T. Yang and W. Huang, *Dalton Trans.*, **2013**, *42*, 12403.
3. H. F. Jiu, G. D. Liu, Z. J. Zhang, Y. H. Fu, J. C. Chen, T. Fan and L. X. Zhang, *J. Rare Earths*, **2011**, *29*, 741.
4. S. S. Zhou, X. Xue, J. F. Wang, Y. Dong, B. Jiang, D. Wei, M. L. Wan and Y. Jia, *J. Mater. Chem.*, **2012**, *22*, 22774.
5. K. Nie, C. Wang, Y. Han, J. Zhang and Y. Yao, *Inorg. Chim. Acta*, **2017**, *466*, 228.

6. S. S. Kelkar, L. Xue, S. R. Turner and T. M. Reineke, *Biomacromolecules*, **2014**, *15*, 1612.
7. C. Zhao, Y. Sun, J. Ren and X. Qu, *Inorg. Chim. Acta*, **2016**, *452*, 50..
8. D. N. Woodruff, R. E. P. Winpenny and R. A. Layfield, *Chem. Rev.*, **2013**, *113*, 5110.
9. Z. Li, X. Li and S. Zheng, *Inorg. Chem. Commun.*, **2017**, *80*, 27.
10. D. A. Joshi, A. Thamizhavel and S. K. Dhar, *Phys. Rev. B*, **2009**, *79*, 014425.
11. Y. Janssen, K. W. Dennis, R. Prozorov, P. C. Canfield and R. W. McCallum, *Phys. Rev. B*, **2008**, *77*, 214407.
12. M. Athar, A. M. Qureshi, G. Li, Z. Shi and S. Feng, *Indian J. Chem.*, **2012**, *51A*, 708.
13. P. Wang, R.-Q. Fan, X.-R. Liu, L.-Y.Wang Y.-L. Yang, W.-W. Cao, B. Yang, W. L. J. Hasi, Q. Su and Y. Mu, *CrystEngComm*, **2013**, *15*, 1931.
14. Rigaku (2002), CrystalClear Version 1.35, Rigaku Corporation.
15. Siemens (1994), SHELXTL^{TM} Ver. 5 Reference Manual, Siemens Energy & Automation Inc., Madison, Wisconsin, USA.
16. Q. Tang, S. Liu, Y. Liu, J. Miao, S. Li, L. Zhang, Z. Shi and Z. Zheng, *Inorg. Chem*., **2013**, *52*, 2799.
17. R. Sang and L. Xu, *Chem. Commun*., **2013**, *49*, 8344.
18. J. Gao, X. Xiong, C. Chen, W. Xie, X. Ran, S. Yue, Y. Liu and Y. Cai, *Inorg. Chem. Commun*., **2013**, *31*, 5.
19. M. Holynska and M. Korabik, *Eur. J. Inorg. Chem*., **2013**, *31*, 5469.
20. J. Zhou, W. Shi, N. Xu and P. Cheng, *Cryst. Growth Des.*, **2013**, *13*, 1218.

A. L. Ramirez, K. E. Knope, T. T. Kelley, N. E. Greig, J. D. Einkauf and D. T. de Lill, *Inorg. Chim. Acta*, **2012**, *392*, 46.

21. D. Brown and D. Altermat, *Acta Crystallogr. B*., **1985**, *41*, 244.
22. F. Q. Huang, K. Mitchell and J. A. Ibers, *Inorg. Chem*., **2001**, *40*, 5123.
23. P. Dürichen and W. Bensch, *Eur. J. Solid State Inorg. Chem*., **1997**, *34*, 1187.
24. R. Tillinski, C. Rumpf, C. Näther, P. Duerichen, I. Jess, S. A. Schunk and W. Bensch, *Z. Anorg. Allg. Chem*., **1998**, *624*, 1285.
25. Y. Onuki, A. Umezawa, W. K. Kwok, G.W. Crabtree, M. Nishihara, T. Yamazaki, T. Omi and T. Komatsubara, *Phys. Rev. B*, **1989**, *40*, 11195.
26. T. Kajitani, K. Nagayama and T. Umeda, *J. Magn.Magn. Mater.*, **1992**, *117*, 379.